論文 / 著書情報
Article / Book Information

Title	Ternary composites of linear and hyperbranched polyimides with nanoscale silica for low dielectric constant, high transparency, and high thermal stability
Authors	Seongku KIM, Shinji ANDO, Xiaogong WANG
Citation	RSC Advances, Vol. 5, Issue 50, pp. 40046-40054
Pub. date	2015, 4
Creative Commons	See the 1st page of the article.

RSC Advances

PAPER

View Article Online
View Journal | View Issue

Cite this: *RSC Adv.*, 2015, **5**, 40046

Ternary composites of linear and hyperbranched polyimides with nanoscale silica for low dielectric constant, high transparency, and high thermal stability

Seongku Kim,[a] Shinji Ando*[b] and Xiaogong Wang*[a]

A new series of ternary polyimide–silica composites was developed to obtain polymer films with low dielectric constant, high optical transparency, and good thermal stability. By using a linear polyamic acid with triethoxysilane termini and a hyperbranched polyimide with peripheral hydroxyl groups ($HBPI_{BPADA\text{-}TAP(OH)}$), the ternary composites were fabricated through *in situ* imidization and sol–gel reaction with tetraethoxysilane. The results show that the composite films exhibit significantly improved properties due to the strong silica cross-linkages between organic–inorganic phases. The triethoxysilane termini can effectively enhance transparency because of the homogeneous dispersion of the inorganic phase in the PI matrices and the improved dispersibility through their strong covalent and partial hydrogen bonding with inorganic silica networks. With an appropriate content of 30% $HBPI_{BPADA\text{-}TAP(OH)}$ and 20% SiO_2 in the linear polyimide ($PI_{6FDA\text{-}APB(Si)}$), the dielectric constant (D_k) can reach the lowest value of 2.19 at 100 kHz. The highest transmittance of 96% at 450 nm is obtained for a ternary hybrid containing 20% SiO_2 and 10% $HBPI_{BPADA\text{-}TAP(OH)}$. The incorporation of $HBPI_{BPADA\text{-}TAP(OH)}$ does not cause negative effects on the thermal stability. The ternary hybrid containing 20% SiO_2 and 10% $HBPI_{BPADA\text{-}TAP(OH)}$ also exhibits the lowest coefficient of thermal expansion (CTE) of 27.8 ppm $°C^{-1}$, when compared with 29.9 ppm $°C^{-1}$ for the binary composite as $PI_{6FDA\text{-}APB(Si)}$ with 20% SiO_2. These properties can well match the requirements for potential applications in the microelectronics insulator fields as interlayer dielectrics of advanced electronic devices.

Received 24th March 2015
Accepted 27th April 2015

DOI: 10.1039/c5ra05227k

www.rsc.org/advances

Introduction

Insulating interlayer materials possessing low dielectric constant, high transparency, and thermal stability are urgently demanded in the microelectronics industry. The low dielectric constant is required to accelerate signal transmission by reducing resistance capacitance (RC) delay time among the chips in large integrated circuit or multilayer printed circuit boards, and to alleviate power dissipation by reducing capacitance between interconnection conductor lines.[1] For improving the insulating and electronic transmission properties of flexible wiring boards, it is of particular interests in developing organic–inorganic composites. Based on polyimides (PIs) with the reduced dielectric constant, organic–inorganic binary composites have been reported as a promising system for possible applications in high-speed, high-frequency circuits in electric material fields.[1–6]

Since it was reported by Kim and Webster in 1990,[7] hyperbranched polymers have received much attention in a variety of fields,[2,6,8,9] because of the unique properties, such as low solution viscosity, high solubility, increasing free volume, as compared with their linear analogues. Their highly branched structures with a large number of terminated functional groups are highly characteristic features for some specific application fields. Particularly, it can be used as an efficient component to enhance the interaction between the organic and inorganic phases through covalent and hydrogen bonding.

In the past decade, hyperbranched polyimides (HBPIs) have been studied from various aspects, such as synthesis,[10] characterization,[11] gas permeability,[10,12–14] hydrogen storage,[6] nonlinear optics,[15] and optoelectronics.[16] One unique feature of the hyperbranched structures is the existence of many open and accessible cavities (typically several angstroms in size) in a rigid branched structure.[14,15,17] This unique feature can result in air gap or pore voids systems,[8,18] low polarization effects,[19–21] and increased free volume.[6,18–20,22] These characteristics can be used

[a]*Department of Chemical Engineering, Laboratory of Advanced Materials (MOE), Tsinghua University, Beijing, 100084, P. R. China. E-mail: wxg-dce@mail.tsinghua.edu.cn*

[b]*Department of Chemistry & Materials Science, Tokyo Institute of Technology, Ookayama 2-12-1-E4-5, Meguro-ku, Tokyo, 152-8552, Japan. E-mail: sando@polymer.titech.ac.jp*

as a protocol for developing polyimides with low dielectric constant, high optical transparency and thermal stability.

In our previous studies, we have synthesized a hydroxyl-terminated hyperbranched polyimide ($HBPI_{BPADA\text{-}TAP(OH)}$) and developed a series of ternary composites by using a typical linear polyimide, $HBPI_{BPADA\text{-}TAP(OH)}$ and SiO_2.[23,24] Owing to particular features of hyperbranched polymers, such as a large number of end groups, high solubility, increased free volume and high reactivity, the ternary composites show significantly improved properties, such as low dielectric constant, high transparency and thermal stability. However, the linkage between the linear PI and inorganic particles has not been considered for the composites.

In this work, we developed a way to enhance the interaction between polyimide backbone and silica phase. We used a linear polyimide with triethoxysilane-terminated group, which has been developed in our recent study for a binary system.[25] To further improve the properties, we fabricated a series of new ternary hybrid composites, $PI_{6FDA\text{-}APB(Si)}$_$HBPI_{BPADA\text{-}TAP(OH)}$_$SiO_2$, by the typical sol–gel method. The structures and properties of the composites were carefully characterized. The ternary hybrid composites not only show significantly reduced dielectric constants, but also exhibit other improved performances such as highly transmittance and good thermal properties.

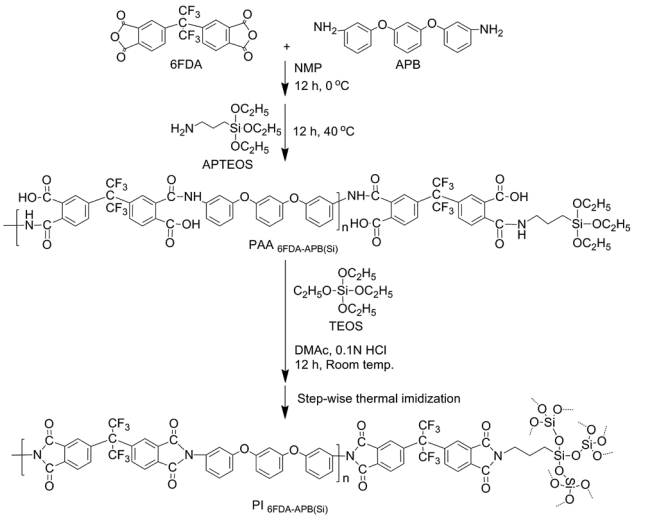

Scheme 1 Synthetic route for $PAA_{6FDA\text{-}APB(Si)}$ and a binary composite (SF-1, $PI_{6FDA\text{-}APB(Si)}$_SiO_2-20%).

Experimental section

Materials

4,4′-(Hexafloroisopropylidene) diphthalic anhydride (6FDA, 95%), 2,4,6-triaminopyrimidine (TAP, 98%), 1,3-bis(3-aminophenoxy)benzene (APB, 98%), and (3-aminopropyl) triethoxysilane (APTEOS, 98%) were purchased from Adamas-Reagent Co. Ltd. 4,4′-Bis(4,4′-isopropylidene diphenoxy) bis-(phthalic anhydride) (BPADA 97%) was purchased from Sigma-Aldrich Corporation. 4-Amino-phenol was purchased from Tianjin Chem. Eng. Lab. *N*, *N*-Dimethylacetamide (DMAc, 98%), *N*, *N*-dimethylmethanamide (DMF, 98%), tetrahydrofuran (THF, 98%), and toluene, used as the reaction media, were purchased from Beijing Chemical Works and Alfa Aesar. The solvent *N*-methyl-2-pyrrolidone (NMP, 97%) was purchased from Beijing Modern Eastern Fine Chemical. Hydrochloric acid (HCl) and tetraethoxysilane (TEOS, 98%) were purchased from Alfa Aesar and used without further purification. If it is not mentioned specifically, the reactants and solvents were used as received without further purification.

Synthesis

The synthetic routes of the materials are shown in Schemes 1 and 2, which show preparations of $PAA_{6FDA\text{-}APB(Si)}$ and its binary composite with silica network (Scheme 1), and the hybrid ternary $PI_{6FDA\text{-}APB(Si)}$_$HBPI_{BPADA\text{-}TAP(OH)}$_$SiO_2$ composite films (Scheme 2). The hydroxyl terminated hyperbranched polyimide ($HBPI_{BPADA\text{-}TAP(OH)}$) was synthesized by the $A_2 + B_3$ polycondensation,[23,26,27] which has been described in our previous report.[23] The preparation details are described below.

Linear polyamic acid with triethoxysilane termini ($PAA_{6FDA\text{-}APB(Si)}$). Polyamic acid (PAA) was synthesized by a typical two-step condensation process at 0 °C. Then, APTEOS was added into the PAA solution to obtain a triethoxysilane terminated PAA. 1,3-Bis(3-aminophenoxy)benzene (APB, 0.526 g, 1.8 mmol) was dissolved in NMP (10 wt%) and cooled in an ice bath, followed by adding 4,4′-(hexaflioroisopropylidene) diphthalic anhydride (6FDA, 1 g, 2.25 mmol) under stirring. Then, (3-aminopropyl) triethoxysilane (APTEOS, 0.199 g, 0.9 mmol) was slowly dropped into the mixture. The molar ratio of 6FDA : APB : APTEOS was controlled to be 5 : 4 : 2. After stirring at 40 °C for 12 h, the PAA solution with silica terminated groups ($PAA_{6FDA\text{-}APB(Si)}$) was obtained. FT-IR (KBr, cm^{-1}): 3450 cm^{-1} (–CONH); 2920 cm^{-1} (C–CH_2–C); 1690 cm^{-1} (C═O, –COOH); 1629 cm^{-1} (C═O, –CONH); 1021 cm^{-1} (–Si–O–C_2H_5).

$PI_{6FDA\text{-}APB(Si)}$_SiO_2-20% binary composite (SF-1). SF-1 was prepared by hydrolysis reaction with TEOS (theoretical SiO_2 content of 20 wt%) and heated through several steps up to the highest temperature to obtain the binary composites.[25] The preparation of the binary composite is given here as a typical example. Stoichiometric quantities of TEOS in DMAc (10 wt%, 1.38 g), and HCl in deionized water (0.1 N, 0.048 g) were mixed and stirred at room temperature for 0.5 h to form the SiO_2 sol. Then, the SiO_2 sol was added to the $PAA_{6FDA\text{-}APB(Si)}$ solution (10 wt%, 2 g) by droplets under stirring. The mixture was then stirred at room temperature for 6 h and $PAA_{6FDA\text{-}APB(Si)}$_$SiO_2$-20% precursor was obtained. In the second stage, the $PAA_{6FDA\text{-}APB(Si)\ (Si)}$_$SiO_2$-20% precursor solution was casted on the glass plate and heated at 80 °C for 2 h. The film was then thermally imidized by step-wise heating at 150 °C (1 h), 200 °C (1 h), and 300 °C (1 h) to afford the $PI_{6FDA\text{-}APB(Si)}$_SiO_2-20% binary composite. FT-IR (KBr, cm^{-1}): 2920 cm^{-1} (C–CH_2–C); 1776 cm^{-1} (C═O *sym.* str. imide.); 1716 cm^{-1} (C═O *asym.* str. imide.); 1587 cm^{-1} (CC str. Ar.); 1477 cm^{-1} (C–CH_2–C); 1443 cm^{-1} (C═C str. Ar.); 1364 cm^{-1} (C–N–C str. imide.); 1296 cm^{-1} (–CF_3); 1235–1192 cm^{-1} (Ar.–O–Ar.); 1125 cm^{-1} (–CF_3); 1096–1067 cm^{-1}

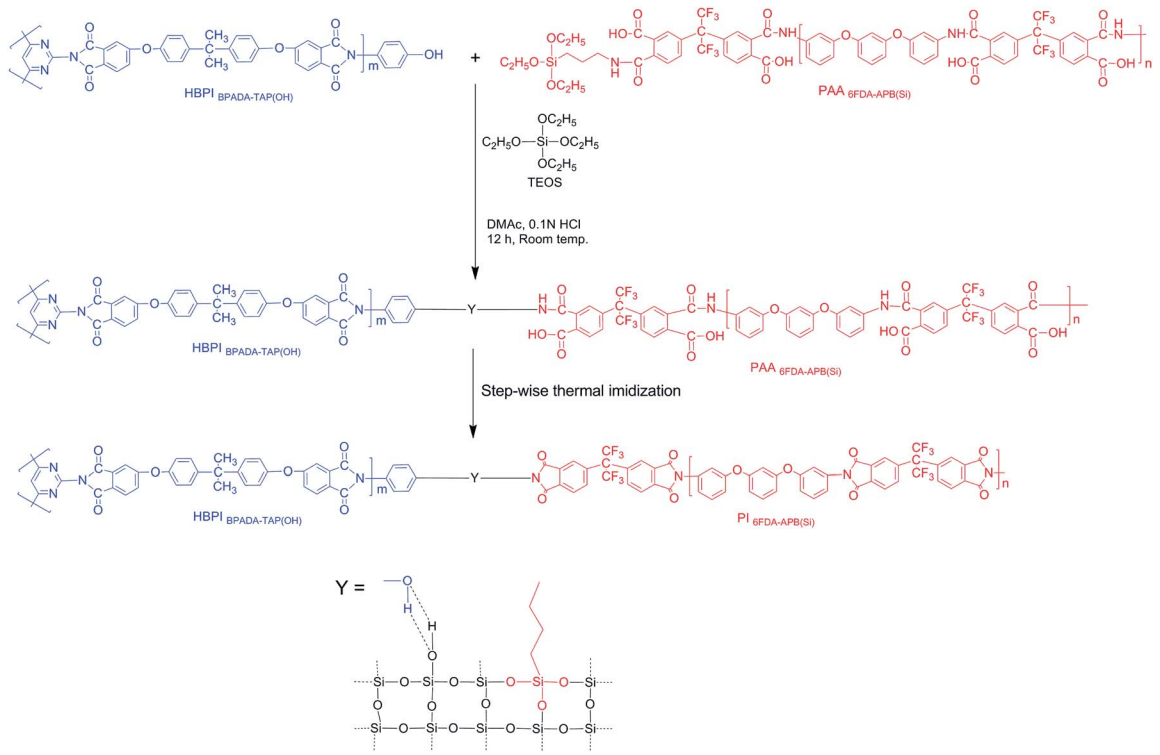

Scheme 2 Synthetic route for PI $_{6FDA\text{-}APB(Si)}$_HBPI$_{BPADA\text{-}TAP(OH)}$_SiO_2 hybrid ternary composite.

(Si–O–Si), 964 cm^{-1} (subst. Ar.); 888 cm^{-1} (Si–OH); 845–718 cm^{-1} (subst. Ar.); 680 cm^{-1} (–CF_3); 3500–3300 cm^{-1} and 1300 cm^{-1} (non amine structure band, –NH_2); 3350 cm^{-1} (non amide band, –NH–); and 1690–1629 cm^{-1} (non PAA structure band).

$PI_{6FDA\text{-}APB(Si)}$_$HBPI_{BPADA\text{-}TAP(OH)}$-10–40%_$SiO_2$-20% (SF-2–5) hybrid ternary composites. The ternary hybrid composite films were prepared by a typical sol–gel method (Scheme 2). The preparation procedures for a composite SF-3 ($PI_{6FDA\text{-}APB(Si)}$_$HBPI_{BPADA\text{-}TAP(OH)}$-20%_$SiO_2$-20%) is given here as a typical example. Stoichiometric quantities of TEOS in DMAc (10 wt%, 1.38 g), and HCl in deionized water (0.1 N, 0.048 g) were mixed and stirred at room temperature for 0.5 h to form the SiO_2 sol. Then, the SiO_2 solution was added dropwise into the mixture solution of linear $PAA_{6FDA\text{-}APB(Si)}$ (10 wt%, 2 g) and $HBPI_{BPADA\text{-}TAP(OH)}$ (0.04 g) under stirring. The solution was stirred at room temperature for 12 h to obtain the precursor. In the second stage, the precursor solution was casted on the glass plate and heated at 80 °C for 2 h. The film was then thermally imidized by stepwise heating at 150 °C (1 h), 200 °C (1 h), and 300 °C (1 h).

The hybrid ternary composites with different compositions were prepared by a similar method by adjusting the composition of the $PI_{6FDA\text{-}APB(Si)}$ and silica. The film formation property of the hybrid ternary composite depended on the contents of the $HBPI_{BPADA\text{-}TAP(OH)}$ and TEOS. By using the linear $PAA_{(Si)}$ and hyperbranched polyimide, the hybrid ternary composites were prepared successfully. The films are named as SF-2 to SF-5 ($PI_{6FDA\text{-}APB(Si)}$_$HBPI_{BPADA\text{-}TAP(OH)}$-10–40%_$SiO_2$-20%). The percentage given in the generic abbreviations are the weight percentage. The hybrid films exhibit similar spectra, the characteristic IR absorption bands are listed below.

[SF-2–SF-5] FTIR (KBr, cm^{-1}): 2920 cm^{-1} (C–CH_2–C); 2911 cm^{-1} (–CH_3 *sym.* str. Al.); 1766 cm^{-1} (C=O *sym.* str. imide.); 1716 cm^{-1} (C=O *asym.* str. imide.); 1587 cm^{-1} (C=C str. Ar.); 1504 cm^{-1} (*asym.* tri-subst. Ar.); 1477 cm^{-1} (C–CH_2–C); 1443 cm^{-1} (C=C str. Ar.); 1364 cm^{-1} (C–N–C str. imide.); 1356 cm^{-1} (–CH_3 Al.); 1296 cm^{-1} (–CF_3); 1235–1192 cm^{-1} (Ar.–O–Ar.); 1125 cm^{-1} (–CF_3); 1096–1067 cm^{-1} (Si–O–Si), 1012 cm^{-1} (*para*-di-subst. Ar.); 964 cm^{-1} (subst. Ar.); 888 cm^{-1} (Si–OH); 845 cm^{-1} (subst. Ar.); 680 cm^{-1} (–CF_3); and 1690–1629 cm^{-1} (non PAA structure band).

Characterization

Fourier transform infrared (FTIR) spectroscopic measurements were performed using a Magna-IR Nicolet 560 in the range 4000–450 cm^{-1} at a resolution of 0.35 cm^{-1} by incorporating samples in KBr disks. The phase transitions and thermal properties were characterized by differential scanning calorimeter (DSC), thermal gravimetric analysis (TGA), and dynamic mechanical analysis (DMA). TGA was performed with a TGA 2050 analyzer (TA instrument Co.) at a heating rate of 20 °C from room temperature to 900 °C under nitrogen. Thermal phase transitions of the polymers were scanned by DSC 2910 (TA Instrument Co.) with a heating rate of 20 °C min^{-1} under nitrogen. The dielectric constants were measured using a NOVOCOOL Alpha-ANB (Novocontrol Technologies GmbH & Co. KG) dielectric analyzer with silver paint electrode. The measurements were carried out at the room temperature with

scan frequencies from 1 Hz to 10^6 Hz by a reference of commercial Kapton® HN film (D_k = 3.81 at 100 kHz). The thickness of specimens was controlled to be 17–24 μm. The coefficients of thermal expansion (CTE) parallel to the film surfaces were measured using a DMA Q800 dynamic mechanical analyzer (DMA, TA Instrument Co.) in extension mode over a temperature range from 25 to 320 °C with a force of 0.01 N. The size of samples was 14 mm in length, 5 mm in width, and 2227 μm in thickness. UV-visible absorption spectra of films were measured on a Lamba Bio-40 spectrometer (Perkin-Elmer). A silica glass plate was used as a reference, and the thickness of specimens was below 10 μm. Cross-sectional images of the PI hybrid films were obtained by scanning electron microscopy (SEM) using a S5500 microscope (Hitachi) operating at an acceleration voltage of 5.0 kV. The cross-sectioned samples were prepared by breaking films in liquid nitrogen and sputtered with carbon nanoparticles.

Results and discussion

Synthesis and characterization

In this study, a series of hybrid nano-composites was prepared. To facilitate the comparison and discussion, the binary composite ($PI_{6FDA\text{-}APB(Si)}$_SiO_2-20%) is referred to as SF-1, and abbreviations SF-2–SF-5 are used to denote the hybrid ternary composites $PI_{6FDA\text{-}APB(Si)}$_$HBPI_{BPADA\text{-}TAP(OH)}$-10–40%_$SiO_2$-20%.

FT-IR spectra of $HBPI_{BPADA\text{-}TAP(OH)}$, SF-1 and ternary hybrid composites SF-2–SF-5 are shown in Fig. 1. In the spectra of $HBPI_{BPADA\text{-}TAP(OH)}$ and all the composites, the absorption bands assignable to imide structure are clearly observed at 1785, 1766 and 1731, 1716 cm^{-1} for the symmetric and anti-symmetric stretching vibrations of the carbonyl groups, and there are no obvious absorption bands of polyamic acid (PAA) between 1690 and 1629 cm^{-1}. All composites clearly exhibit typical spectral characteristics related to the SiO_2 network formation. A very weak absorption at 888 cm^{-1} (Si–OH) and strong absorption at 1096–1067 cm^{-1} (Si–O–Si, symmetric stretching vibrations) in all the composites indicate that only tiny amount of Si–OH groups still remains and dominant Si–O–Si networks form during the hydrolysis of alkoxy groups. In Fig. 1 and 2, the absorption bands of $–CH_2–CH_2–$ linkage from APTEOS are clearly observed at 2920 and 1477 cm^{-1}. There are no obvious absorption bands of amine ($–NH_2$) at 3500–3300 cm^{-1} and 1300 cm^{-1}, and –NH– at 3450 cm^{-1} after the terminal reaction with APTEOS. It proves that the linkage is successfully introduced between linear PI backbone and silica network.

The FT-IR spectra of SF-1 to SF-5 show significant shifts for the absorption bands related with the transformation during the synthesis of the hybrid ternary composites. The absorption bands of C=O are shifted from 1785 and 1731 cm^{-1} for $HBPI_{BPADA\text{-}TAP(OH)}$ to 1766 and 1716 cm^{-1} for the hybrid ternary composites. The absorption band of C–N is also shifted from 1384 cm^{-1} for $HBPI_{BPADA\text{-}TAP(OH)}$ to 1364 cm^{-1} for the hybrid

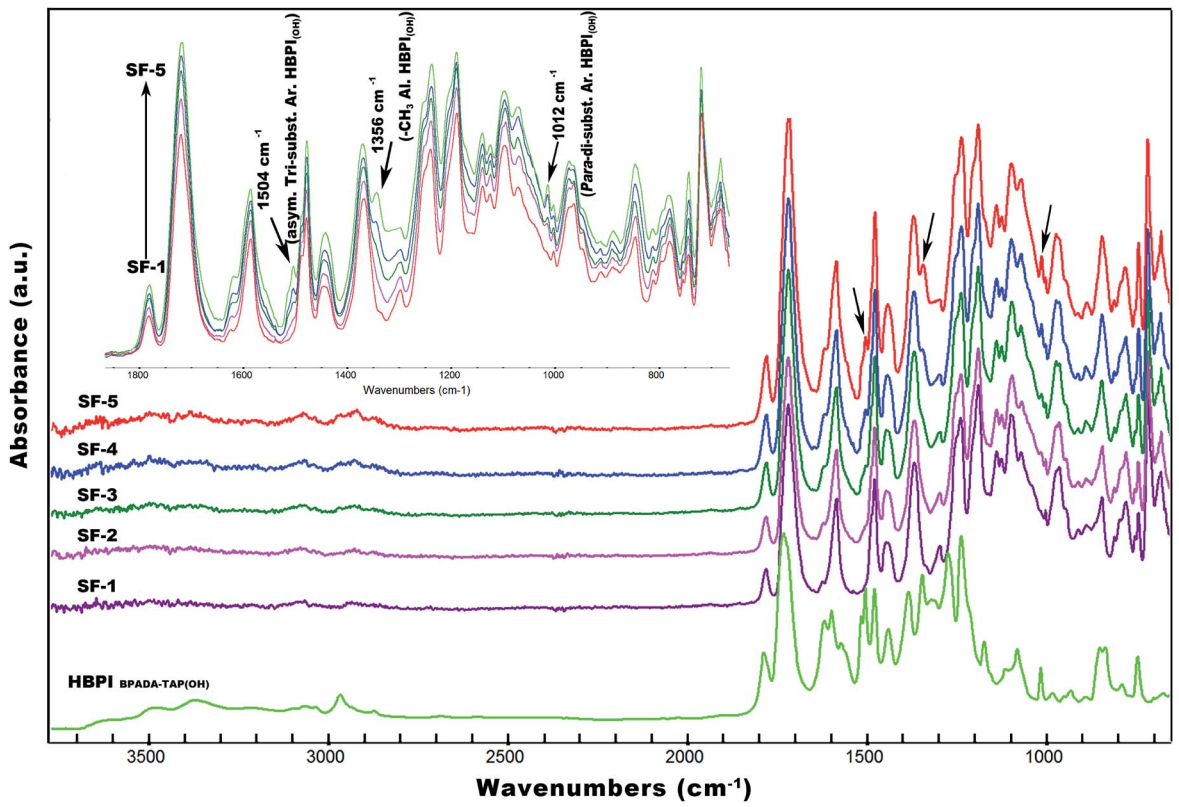

Fig. 1 FTIR spectra of the hydroxyl terminated hyperbranched polyimide, $PI_{6FDA\text{-}APB(Si)}$_SiO_2-20% binary composite (SF-1), and $PI_{(Si)}$_$HBPI_{(OH)}$-10–40%_SiO_2-20% hybrid ternary composites (SF-2–5).

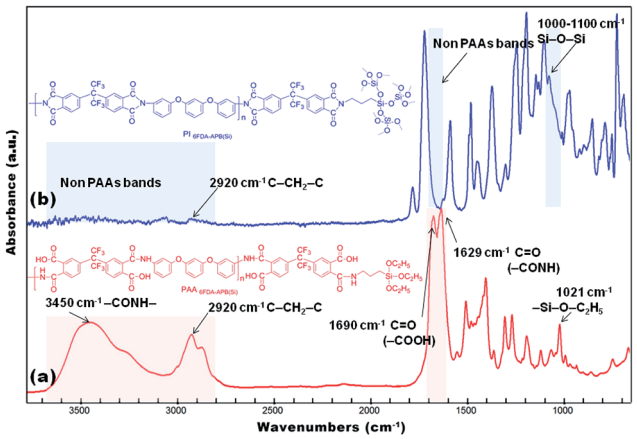

Fig. 2 FTIR spectra of (a) the silica terminated polyamic acids ($PAA_{6FDA\text{-}APB(Si)}$) in NMP solvent, and (b) $PI_{6FDA\text{-}APB(Si)}$–SiO_2-20% binary composite (SF-1).

ternary composites. These band-shifts are related with the hydrogen bonding and hydrolysis reactions with TEOS,[28] which effectively enhance the intermolecular interactions. Therefore, with the increase of the $HBPI_{BPADA\text{-}TAP(OH)}$ percentage, the characteristic bands of C=O and C–N are gradually shifted to lower wavenumbers. Moreover, the intensities of the absorption bands around 1776, 1716 (C=O stretching vibrations), 1504 (tri-substituted aromatic benzene), 1364 cm^{-1} (C–N stretched imide), 1356 cm^{-1} (aliphatic methyl groups), and 1012 cm^{-1} (*para*-di-substituted aromatic benzene) increase with the increase of the $HBPI_{BPADA\text{-}TAP(OH)}$ amount by using the intensity of SiO_2 as the standard.

Above results all verify that, not only the PAA precursor is completely converted to PI, but also SiO_2 networks are formed in the organic–inorganic composite through the sol–gel process.

Dielectric properties of hybrid binary and ternary composites

The dielectric constants of the unary PI (S-1), composites (SF-1–5) and commercial Kapton® HN as a control are shown in Fig. 3 and also listed in Table 1. The dielectric constants (D_k) of the composite films and related materials were measured in the frequency range from 1 Hz to 10^6 Hz at a fixed frequency (100 kHz).

The dielectric constants show an increase with decreasing frequency, which is a typical frequency dependence of dielectric properties.[29] It can be described by Cole–Cole equation,[30]

$$\varepsilon^* - \varepsilon_\infty = (\varepsilon_0 - \varepsilon_\infty)/[1 + (i\omega\tau_0)^{1-\alpha}] \quad (1)$$

where ε^* is the complex dielectric constant, ε_0 and ε_∞ are the dielectric constants at "static" and "infinite frequency", $\omega = 2\pi$ times the frequency, and τ_0 is a generalized relaxation time. The exponent parameter α can assume a certain value between 0 and 1, in which the former case corresponds to the result by Debye for polar dielectrics.[30]

The dielectric constants of the films prepared in this study are significantly lower than that of the linear $PI_{6FDA\text{-}APB}$ (S-1).[23] Compared with the three series of PI composites SA, SB, and SC

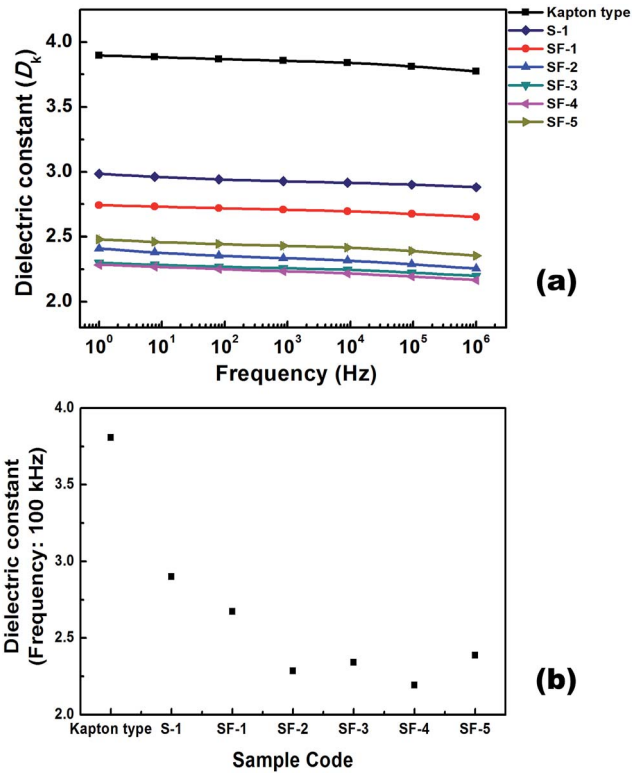

Fig. 3 Dielectric constant (D_k) of the $PI_{6FDA\text{-}APB}$ unary PI (S-1), $PI_{6FDA\text{-}APB(Si)}$–SiO_2-20% binary composite (SF-1), and $PI_{(Si)}$–$HBPI_{(OH)}$-10–40%–SiO_2-20% hybrid ternary composites (SF-2–5); (a) scanning frequency from 1 Hz to 10^6 Hz, (b) fixed frequency of 100 kHz.

groups reported by us,[23,24] the dielectric constants of the series SF composites are obviously reduced, and they are also less dependent on the frequency. Especially, the decrease of D_k in the 1 Hz to 10^3 Hz range shown in Fig. 3(a) could be related to a decrease in space charge polarization between organic and inorganic phases.[23–25] It verifies in comparison to series SA that the series SF composites has good adhesion between the silica and PI matrix due to the terminated linkages on $PI_{6FDA\text{-}APB(Si)}$ and reaction of $HBPI_{BPADA\text{-}TAP(OH)}$ with TEOS. The D_k values of hybrid ternary composites (SF-2–SF-5) are smaller than that of the binary composite (SF-1). Under the optimized conditions, SF-4 exhibits the lowest D_k of 2.19, which is slightly smaller than SA-4 (a typical specimen in SA series, $D_k = 2.24$).[23] It can be attributed to that the terminated linkage of $PI_{6FDA\text{-}APB(Si)}$ to promote the homogeneous dispersion, and miscibility through their strong covalent bonds. And it enhances the effect of $HBPI_{BPADA\text{-}TAP(OH)}$ on reducing D_ks by forming Si–O–Si with the inorganic phase. The low dielectric constants of the system are also related with the fundamental characters of monomers, *i.e.*, the high fluorine content of 6FDA,[31,32] the flexible and bent structure of APB,[33,34] and the bulky side groups of BPADA.[35–37] Moreover, the introduction of inorganic silica effectively reduces the moisture absorption of the material and expands the free volume.[29] The improved phase dispersion of $HBPI_{BPADA\text{-}TAP(OH)}$ and $PI_{6FDA\text{-}APB(Si)}$ plays a very important role to result in the reduced dielectric constant in hybrid ternary composite films.

Table 1 Dielectric, optical, and thermal properties of $PI_{6FDA\text{-}APB(Si)}$_SiO_2-20% (SF-1) and $PI_{6FDA\text{-}APB(Si)}$_$HBPI_{BPADA\text{-}TAP(OH)}$-10–40% (SF-2–5) hybrid ternary composite films

			Transmittance			DSC	TGA			
Sample	Thickness[a] μm	D_k[b]	λ_{cutoff} nm	450 nm/ %	400 nm/ %	T_g/ °C	$T_d^{c5\%}$/ °C	$T_d^{c10\%}$/ °C	R_{w800}[d]/ %	CTE[e] ppm °C^{-1}
SF-1 $PI_{(Si)}$_SiO_2-20%	24	2.67	326	87	68	203.3	529	545	52	29.9
SF-2 $PI_{(Si)}$_$HBPI_{(OH)}$-10%_SiO_2-20%	17	2.28	326	96	92	207.4	527	546	52	27.8
SF-3 $PI_{(Si)}$_$HBPI_{(OH)}$-20%_SiO_2-20%	20	2.22	326	94	86	206.6	513	540	51	27.9
SF-4 $PI_{(Si)}$_$HBPI_{(OH)}$-30%_SiO_2-20%	20	2.19	325	94	86	210.8	494	531	52	28.4
SF-5 $PI_{(Si)}$_$HBPI_{(OH)}$-40%_SiO_2-20%	21	2.39	326	88	75	203.8	492	526	51	32.9

[a] The thickness of specimens for dielectric constant measurement. [b] Measured dielectric constant at a frequency of 100 kHz. [c] Temperatures at which 5% and 10% weight loss occurred, respectively, measured by TGA at a heating rate of 20 °C min^{-1} and a N_2 gas flow rate of 25 cm^3 min^{-1}. [d] Residual weight percentages at 800 °C. [e] The coefficients of thermal expansion (CTE) at the temperature range from 100 to 150 °C with a force of 0.01 N.

Morphology of hybrid binary and ternary composites

Fig. 4 shows typical SEM images of the representative composite films. It is confirmed by the SEM observation that $HBPI_{BPADA\text{-}TAP(OH)}$ can reinforce the binding between $PI_{6FDA\text{-}APB(Si)}$ and SiO_2 and promote the dispersion of SiO_2 in the matrices. Fig. 4(a) and (c) show the SEM images of SA-1 ($PI_{6FDA\text{-}APB}$_SiO_2-20%),[23] and SF-1 ($PI_{6FDA\text{-}APB(Si)}$_SiO_2-20%) without the existence of $HBPI_{BAPDA\text{-}TAP(OH)}$. Compared with SA-1, which has been reported in our previous study, the SF-1 still displays aggregated silica particles but shows obviously reduced size of spherical beads with smooth surface. The average size of partially aggregated silica particles reduces from 1500 nm for SA-1 (Fig. 4(a)) to around 100–200 nm for SF-1 (Fig. 4(c)). When the triethoxysilane termini are introduced to the PI, dispersion of SiO_2 in matrices is dramatically improved. This result is consistent with our previous study for optically transparent polyimide.[25]

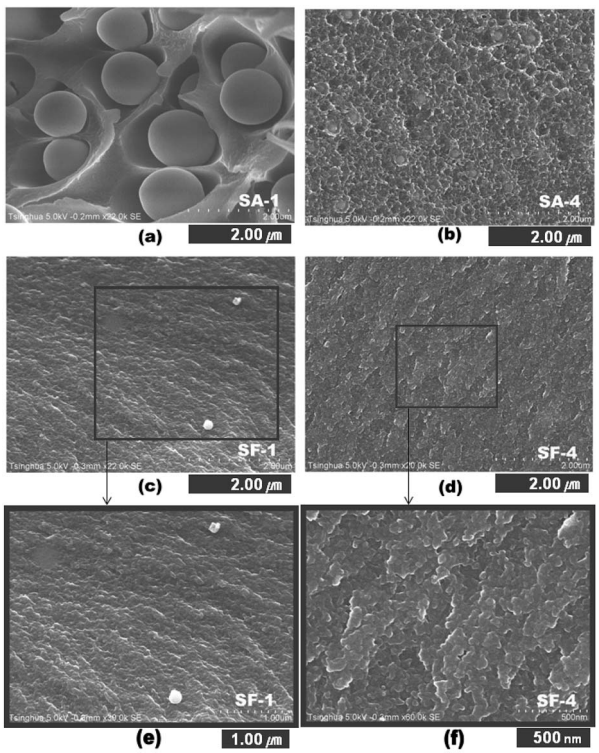

Fig. 4 Typical SEM images of PI and the composites, (a) $PI_{6FDA\text{-}APB}$_SiO_2-20% (SA-1),[23] (b) $PI_{6FDA\text{-}APB}$_$HBPI_{BPADA\text{-}TAP(OH)}$-30%_$SiO_2$-20% (SA-4),[23] (c), (e) $PI_{6FDA\text{-}APB(Si)}$_SiO_2-20% (SF-1), and (d), (f) $PI_{6FDA\text{-}APB(Si)}$_$HBPI_{BPADA\text{-}TAP(OH)}$-30%_$SiO_2$-20% (SF-4); scale bar: 2 μm (a–d), 1 μm (e), and 500 nm (f). Pictures from ref. 23 are reproduced with permission.

For the ternary composites, such as SF-4 incorporating $HBPI_{BPADA\text{-}TAP(OH)}$-30%, SEM images indicate that $HBPI_{BPADA\text{-}TAP(OH)}$ shows obvious effect to further suppress the aggregation of silica (Fig. 4(d)). It can be attributed to the peripheral hydroxyl (–OH) groups, which can form covalent linkages to silica network or hydrogen bonding linkages after the hydrolysis reaction. Therefore, the silica phase in SF-4 can hardly be seen and the smooth surface morphology is remarkably similar with PI without the inorganic phase. Compared with SA-1 and SA-4 of our previous study (Fig. 4(a) and (b)), the synergy of $HBPI_{BPADA\text{-}TAP(OH)}$ and $PI_{6FDA\text{-}APB(Si)}$ can effectively reduce the aggregation of silica and suppress phase separation between heterogeneous organic–inorganic phases. Moreover, the hyperbranched structure can introduce the nano-scaled cavities,[6,8,18] which are beneficial for reducing the dielectric constants the hybrid ternary composites. As discussed in the following sections, owing to the reduced phase separation, the transmittance of the composites can be significantly improved by incorporating $HBPI_{BPADA\text{-}TAP(OH)}$ into the $PI_{6FDA\text{-}APB(Si)}$_SiO_2 binary composite. The decrease in D_k in the frequencies between 1 and 10^3 Hz range, which is mainly form the space charge polarization, can also be attributed to the effective reduction in phase separation.

Optical properties of hybrid binary and ternary composites

The optical transparency of SF-1 and hybrid ternary composites (SF-2–5) was characterized with UV-vis spectroscopy. Fig. 5 shows the UV-vis transmission spectra of the composite films. The cutoff wavelengths (absorption edge, λ_{cutoff}) and the transmittance at 450 nm and 400 nm estimated from these spectra are listed in Table 1.

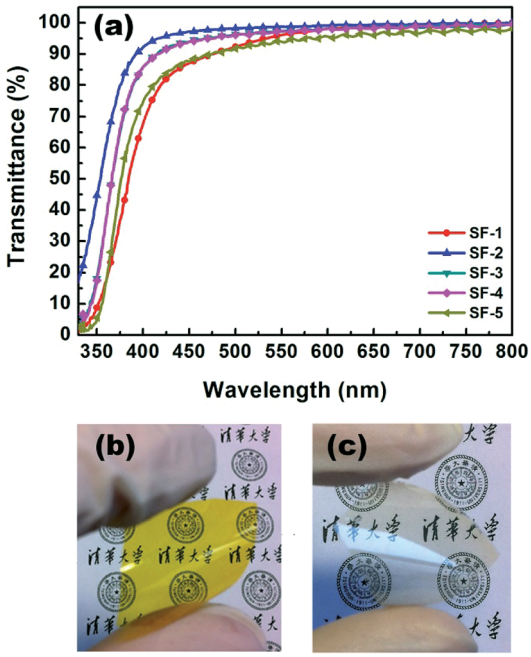

Fig. 5 (a) UV-vis spectra of the $PI_{6FDA\text{-}APB(Si)}$_SiO_2-20% binary composite (SF-1), and $PI_{6FDA\text{-}APB(Si)}$_$HBPI_{BPADA\text{-}TAP(OH)}$-10–40%_$SiO_2$-20% ternary hybrid composites (SF-2–5). The film thickness was under 10 μm on the glass substrates. (b) Commercial Kapton film (25 μm) and (c) SF-2 film (28 μm).

The optical transparency of the series SF composites is obviously improved by incorporating $HBPI_{BPADA\text{-}TAP(OH)}$ into the $PI_{6FDA\text{-}APB(Si)}$_SiO_2 system. On the other hand, the effect of triethoxysilane termini in $PI_{6FDA\text{-}APB\ (Si)}$ is also observed from the improved transparency compared with those of the series SA composites reported by us before.[23] The SF-1 composite exhibits a transmittance of 87% at 450 nm. By incorporating $HBPI_{BPADA\text{-}TAP(OH)}$, SF-2 shows the highest transmittance of 96% at 450 nm. The transmittance of SF-1 is also improved in comparison to SA-1.[25] The composite with the lowest D_k (SF-4) in the series also shows a transmittance of 94% at 450 nm, which are also obviously higher than that of SA-4 ($PI_{6FDA\text{-}APB}$_$HBPI_{BPADA\text{-}TAP(OH)}$-10%_$SiO_2$-20%).[23]

Fundamental characters of monomers, *i.e.*, the high fluorine content of 6FDA,[31,32] the flexible and bent structure of APB,[33,34] and the bulky side groups of BPADA[35–37] are important for the colorless feature. On the other hand, this effect is also attributed to the synergy effect of $HBPI_{BPADA\text{-}TAP(OH)}$ and $PI_{6FDA\text{-}APB(Si)}$ components to reduce the phase separation between PI matrices and silica particles, which improves the dispersibility and reduces the size of silica particles. Therefore, it can reduce the light scattering from the aggregated inorganic silica phase in the visible wavelength scale.

Thermal properties of hybrid binary and ternary composites

The thermal phase transition behavior of the hybrid ternary composites and related materials was investigated by DSC. The results are shown in Fig. 6(a) and summarized at Table 1.

All the hybrid ternary composites and related materials show glass transitions, which means the PI components exist in the amorphous phase. The SF series composites show the glass transition temperatures (T_gs) ranging from 203.3 to 210.8 °C. After incorporating $HBPI_{BPADA\text{-}TAP(OH)}$ into the binary system, the T_g of the hybrid ternary composites become slightly higher in a few degree scale than that of SF-1, which is attributed to the covalent cross-linkages and partial hydrogen linkages in the composites networks. It causes enhanced interaction between PI and inorganic silica phase. However, the differences in T_g from SF-2 to SF-5 are only few degrees. The T_g of SF-5 is 203.8 °C, which is the lowest in the series. $HPPI_{BPADA\text{-}TAP(OH)}$ has a hyperbranched structure with low molecular weight. The lower T_g of SF-5 can be attributed to the large free volume and low T_g of the hyperbranched polymer. On the other hand, as long as its concentration is below the critical value, $HBPI_{BPADA\text{-}TAP(OH)}$ does not separate from the matrices or affect the T_g significantly. The effect for reducing T_g is not obvious for the binary composites. The addition of $HBPI_{BPADA\text{-}TAP(OH)}$ does not show an obvious effect to decrease T_g in the ternary composite system, which has also been observed in our previous study.[23]

The thermal decomposition temperatures of the hybrid ternary composites and related materials measured by TGA analysis are shown in Fig. 6(b) and summarized in Table 1. It can be observed for the SF series, the residual weights of the composites are nearly 100% below 450 °C, which are higher than those of the SA, SB, and SC series reported by us before.[23,24]

The 5% and 10% weight loss temperatures ($T_d^{5\%}$ and $T_d^{10\%}$) of SF-1 are 529 and 545 °C, respectively. The ternary hybrid composites (SF-2–5) show the $T_d^{5\%}$ ranging from 527 to 492 °C and $T_d^{10\%}$ from 546 to 526 °C. These are significantly higher than those for the SA series ($T_d^{5\%}$: 487 to 481 °C).[23]

It can be attributed to cross-linked silica networks with $HBPI_{BPADA\text{-}TAP(OH)}$ and $PI_{6FDA\text{-}APB(Si)}$. The T_d values decrease with the increase in the $HBPI_{BPADA\text{-}TAP(OH)}$ content in the systems, which might be caused by the elimination of water molecules from Si–OH and hydroxyl groups of $HBPI_{BPADA\text{-}TAP(OH)}$ at the high temperatures and lower T_d of $HBPI_{BPADA\text{-}TAP(OH)}$.

The coefficient of thermal expansion (CTE) was characterized by DMA in the direction of film surface of the ternary hybrid composites and related materials. The CTE curves are shown in Fig. 6(c) and the CTE values in the temperature range from 100 to 150 °C are listed in Table 1.

The CTE values of the SF series change from 32.9 to 27.8 ppm $°C^{-1}$. By comparing the CTE values below the T_g, the hybrid composites exhibit significantly smaller CTEs than that of the pristine PI (S-1, 37.1 ppm $°C^{-1}$).[23] The smallest CTE value was obtained for SF-2 (27.8 ppm $°C^{-1}$) in the series. It can be attributed to cross-linkages between the hydroxyl groups of $HBPI_{BPADA\text{-}TAP(OH)}$ and silica termini in the $PI_{6FDA\text{-}APB(Si)}$_SiO_2-20%. However, compared to the CTE of 17.8 ppm $°C^{-1}$ for SA-1 ($PI_{6FDA\text{-}APB}$_SiO_2-20%),[23] the CTE value is obviously higher, which also increase with the further increase of $HBPI_{BPADA\text{-}TAP(OH)}$. This is a negative effect of the triethoxysilane termini of $PI_{6FDA\text{-}APB(Si)}$ compare with $PI_{6FDA\text{-}APB}$, which could increase the inter-chain distances and form nano-scale cavities.[14,15,17] In spite of the incorporation of $HBPI_{BPADA\text{-}TAP(OH)}$, the effect of covalent and hydrogen linkages to reduce the CTE is somehow counterbalanced by the $PI_{6FDA\text{-}APB(Si)}$ component. This tendency can be seen by comparing the CTEs among the series SA and SF groups.

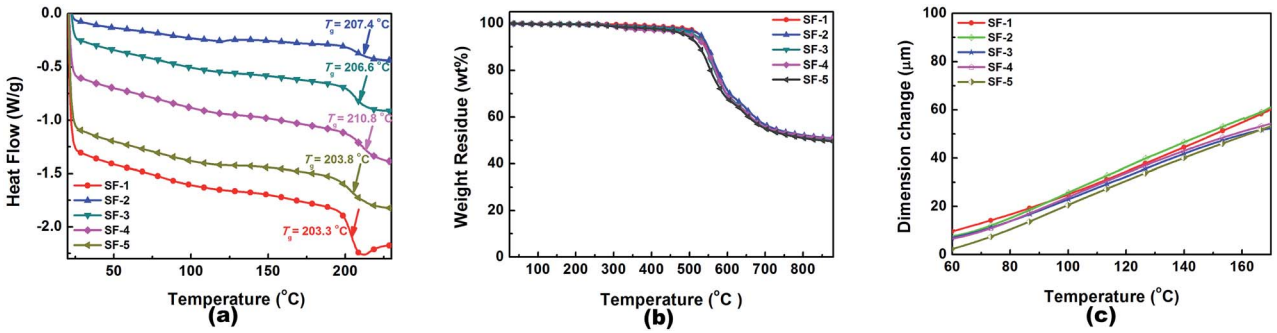

Fig. 6 (a) DSC, (b) TGA, and (c) CTE curves for the $PI_{6FDA\text{-}APB(Si)}$_SiO_2-20% (SF-1) binary composite, and $PI_{6FDA\text{-}APB(Si)}$_$HBPI_{BPADA\text{-}TAP(OH)}$-10–40%_$SiO_2$-20% ternary hybrid composites (SF-2–5).

Even in this case, the CTEs of the ternary hybrid composites are still much smaller than that of typical linear PI (S-1).[23]

Above the results indicate that these hybrid ternary composites show significant improvements in dielectric properties and high transparency, which are attained by introducing $HBPI_{BPADA\text{-}TAP\ (OH)}$ in the $PI_{6FDA\text{-}APB(Si)}$-20% and SiO_2 composite. Although the CTE is reduced by introducing the inorganic silica networks in the ternary system, the triethoxysilane termini of $PI_{6FDA\text{-}APB(Si)}$ is not favorable for further decreasing CTE values.

Conclusion

Based on the linear $PI_{6FDA\text{-}APB(Si)}$ with the triethoxysilane termini and hyperbranched $HBPI_{BPADA\text{-}TAP(OH)}$, ternary hybrid composite films (SF series) were fabricated by sol–gel cross-linking reaction with TEOS. The ternary hybrid composites exhibited desirable dielectric properties. At the appropriate content of $HBPI_{BPADA\text{-}TAP(OH)}$, the dielectric constant (D_k) of SF-4 ($PI_{6FDA\text{-}APB(Si)}$_$HBPI_{BPADA\text{-}TAP(OH)}$-30%_$SiO_2$-20%) showed the lowest value of 2.19 in the series. The optical transparency of the ternary hybrid composite films was also improved because of the synergy effect of $HBPI_{BPADA\text{-}TAP(OH)}$ and $PI_{6FDA\text{-}APB(Si)}$ to reduce the phase separation. The best result was obtained for SF-2 in the ternary hybrid composites, for which the corresponding transmittance was increased from 87% for SF-1 ($PI_{6FDA\text{-}APB(Si)}$_SiO_2-20%) to 96% at the wavelength of 450 nm. The incorporation of $HBPI_{BPADA\text{-}TAP(OH)}$ and $PI_{6FDA\text{-}APB(Si)}$_SiO_2-20% did not cause negative effects on the thermal stability of the binary composites. The CTE of SF-2 ($PI_{6FDA\text{-}APB(Si)}$_$HBPI_{BPADA\text{-}TAP(OH)}$-30%_$SiO_2$-20%, 27.8 ppm $°C^{-1}$) was the lowest in the hybrid ternary composites. The triethoxysilane termini of $PI_{6FDA\text{-}APB(Si)}$ did not show favorable effect to further decrease CTE values. In general, the hybrid ternary composites developed in this study show improved characteristics of dielectric, optical and thermal resistant properties, which is promising to meet the requirements for interlayer dielectrics in advanced electronic devices.

Acknowledgements

The financial support from National Basic Research Program of China (973 Program) under Project 2011CB606102 is gratefully acknowledged.

References

1 W. Volksen, R. D. Miller and G. Dubois, *Chem. Rev.*, 2010, **110**, 56.
2 H. Chen, L. Xie, H. Lu and Y. Yang, *J. Mater. Chem.*, 2007, **17**, 1258.
3 L. Tan, S. M. Liu, F. Zeng, Z. Y. Ling and J. Q. Zhao, *Polym. Adv. Technol.*, 2010, **21**, 435.
4 Y. H. Zhang, Z. M. Dang, J. H. Xin, W. A. Daoud, J. H. Ji, Y. Y. Liu, B. Fei, Y. Q. Li, J. T. Wu, S. Y. Yang and L. F. Li, *Macromol. Rapid Commun.*, 2005, **26**, 1473.
5 Y. H. Zhang, S. G. Lu, Y. Q. Li, Z. M. Dang, J. H. Xin, S. Y. Fu, G. T. Li, R. R. Guo and L. F. Li, *Adv. Mater.*, 2005, **17**, 1056.
6 J. C. Huang, P. C. Lim, L. Shen, P. K. Pallathadka, K. Y. Zheng and C. B. He, *Acta Mater.*, 2005, **53**, 2395.
7 Y. H. Kim and O. W. Webster, *J. Am. Chem. Soc.*, 1990, **112**, 4592.
8 G. F. Zhao, T. Ishizaka, H. Kasai, M. Hasegawa, T. Furukawa, H. Nakanishi and H. Oikawa, *Chem. Mater.*, 2009, **21**, 419.
9 D. J. Massa, K. A. Shriner, S. R. Turner and B. I. Voit, *Macromolecules*, 1995, **28**, 3214.
10 T. Suzuki and Y. Yamada, *J. Polym. Sci., Part B: Polym. Phys.*, 2006, **44**, 291.
11 K. L. Wang, M. Jikei and M. Kakimoto, *J. Polym. Sci., Part A: Polym. Chem.*, 2004, **42**, 3200.
12 T. Suzuki, Y. Yamada and K. Itahashi, *J. Appl. Polym. Sci.*, 2008, **109**, 813.
13 T. Suzuki, Y. Yamada and Y. Tsujita, *Polymer*, 2004, **45**, 7167.
14 T. Suzuki and Y. Yamada, *High Perform. Polym.*, 2007, **19**, 553.
15 Y. J. Lee, J. M. Huang, S. W. Kuo and F. C. Chang, *Polymer*, 2005, **46**, 10056.
16 Y. Ren and D. C. C. Lam, *J. Electron. Mater.*, 2008, **37**, 955.
17 T. Seçkin, S. Köytepe and H. I. Adıgüzel, *Mater. Chem. Phys.*, 2008, **112**, 1040.
18 V. E. Yudin, J. U. Otaigbe, S. Gladchenko, B. G. Olson, S. Nazarenko, E. N. Korytkova and V. V. Gusarov, *Polymer*, 2007, **48**, 1306.
19 E. Hamciuc, C. Hamciuc and M. Olariu, *Polym. Eng. Sci.*, 2009, **50**, 520.
20 Y. T. Chern and J. Y. Tsai, *Macromolecules*, 2008, **41**, 9556.

21 H. Deligöz, S. Özgümüş, T. Yalçınyuva, S. Yildirim, D. Deger and K. Ulutas, *Polymer*, 2005, **46**, 3720.
22 H. W. Wang, R. X. Dong, H. C. Chu, K. C. Chang and W. C. Lee, *Mater. Chem. Phys.*, 2005, **94**, 42.
23 S. K. Kim, X. Y. Wang, S. Ando and X. G. Wang, *RSC Adv.*, 2014, **4**, 27267.
24 S. K. Kim, X. Y. Wang, S. Ando and X. G. Wang, *RSC Adv.*, 2014, **4**, 42737.
25 S. K. Kim, X. Y. Wang, S. Ando and X. G. Wang, *Eur. Polym. J.*, 2015, **64**, 206.
26 J. Hao, M. Jikei and M. Kakimoto, *Macromolecules*, 2002, **35**, 5372.
27 P. J. Flory, *J. Am. Chem. Soc.*, 1952, **74**, 2718.
28 H. Zhou, S. Wu and J. Shen, *Chem. Rev.*, 2008, **108**, 3893.
29 J. O. Simpson and A. K. St. Clair, *Thin Solid Films*, 1997, **308–309**, 480.
30 K. S. Cole and R. H. Cole, *J. Chem. Phys.*, 1941, **9**, 341.
31 G. Hougham, G. Tesoro and J. Shaw, *Macromolecules*, 1995, **27**, 3642.
32 A. E. Feiring, B. C. Auman and E. R. Wonchoba, *Macromolecules*, 1993, **26**, 2779.
33 G. C. Eastmond and J. Paprotny, *Macromolecules*, 1995, **28**, 2140.
34 Y. Imai, *High Perform. Polym.*, 1995, **7**, 337.
35 Y. T. Chern and H. C. Shiue, *Macromolecules*, 1997, **30**, 4646.
36 L. J. Mathias, A. V. G. Muir and V. R. Reichert, *Macromolecules*, 1991, **24**, 5232.
37 X. T. Han, Y. Tian, L. H. Wang and C. F. Xiao, *J. Appl. Polym. Sci.*, 2008, **107**, 618.